



Лаборатория информационных технологий им. М.Г.Мещерякова

Modeling of Physical Processes in Dense and Hot Nuclear Medium

Yu. L. Kalinovsky

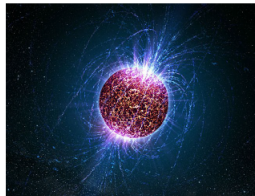
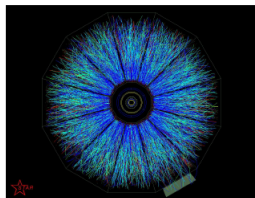
Content

- 1 Introduction
- 2 Mesons at finite temperature in the Nambu – Jona-Lasinio model
- 3 Results and conclusion
- 4 Strange matter and kaon to pion ratio in SU(3) PNJL model
- 5 PNJL Model
- 6 Results and discussion

Why is finite T/μ physics (\approx QCD) interesting?

High energy physics applications

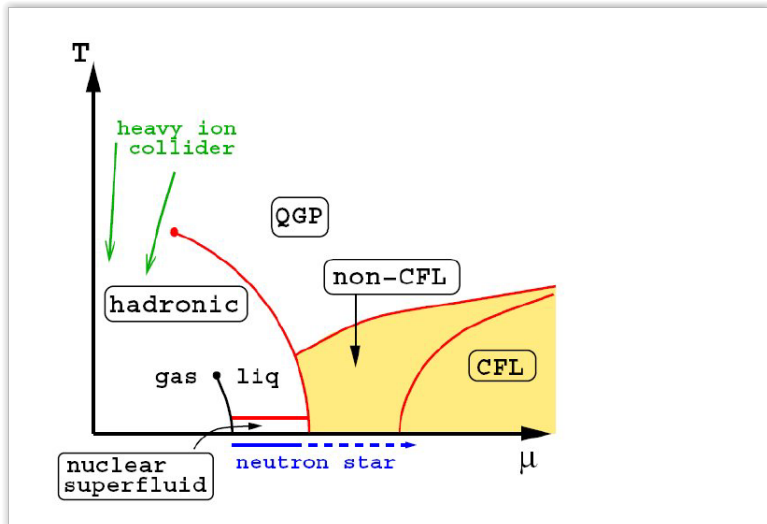
- Heavy ion experiments \Rightarrow Need quantitative understanding of non-Abelian plasmas at
 - High T and small/moderate μ
 - Moderately large couplings
 - In and (especially) out of equilibrium
- Early universe thermodynamics
 - Signatures of phase transitions
 - EW baryogenesis
- Neutron star interiors
 - EoS at high μ and $T \simeq 0$
 - Transport in nucl. matter



Challenges in thermal QCD

To understand heavy ion experiments / early universe thermodynamics want to know (among other things):

- Structure of QCD phase diagram: Phase structure, location of transition lines, critical points,...
- Properties of phase transitions, in particular the deconfinement transition
- Equation of state and other equilibrium quantities



$$\begin{aligned}
 S_{\text{eff}}[q, \bar{q}] = & \int dx_1 dx_2 \bar{q}_A(x_1) [G_0^{-1}(x_1, x_2)]_{AB} q_B(x_2) \\
 & - \frac{1}{2} \int dx_1 dx_2 dy_1 dy_2 [\bar{q}_A(x_1) q_B(y_1)] \\
 & \times [\mathcal{K}^\eta(x_1, y_1; x_2, y_2)]_{AB;CD} [\bar{q}_C(x_2) q_D(y_2)].
 \end{aligned}$$

We employ here the NJL model with two flavours of quarks defined by the Lagrangian

$$\begin{aligned} \mathcal{L}_{\text{NJL}} = & \bar{q} (i\gamma_\mu \partial^\mu - \hat{m}_0) q + G_s \left[(\bar{q}q)^2 + (\bar{q}i\gamma_5 \vec{\tau}q)^2 \right] \\ & - G_v \left[(\bar{q}\gamma^\mu \tau^a q)^2 + (\bar{q}\gamma^\mu \gamma^5 \tau^a q)^2 \right], \end{aligned}$$

with chirally symmetric four-quark interactions in the scalar, pseudo-scalar, vector and axial-vector channels. G_s and G_v are the scalar and vector coupling constants, \bar{q} and q - the quark spinor fields, \hat{m}_0 is the diagonal matrix of the current quark mass, $\hat{m}_0 = \text{diag}(m_u^0, m_d^0)$ with $m_u^0 = m_d^0 = m_0$, and $\vec{\tau}$ are the SU(2) Pauli matrices in flavor space with the components τ^a ($a = 1, 2, 3$).

In the mean-field approximation the constituent quark mass is obtained by solving the gap equation

$$m = m_0 + 8G_s N_c N_f \int_{\Lambda} \frac{d^3p}{(2\pi)^3} \frac{m}{E_p} [1 - f(E^+) - f(E^-)] ,$$

where the dependence on temperature and chemical potential is modeled in the Fermi-functions $f(E^\pm) = (1 + e^{\beta E_p^\pm})^{-1}$ and the quark (anti-quark) energy dispersion relation $E_p^\pm = E_p \pm \mu$.

Mesons are considered as quark-antiquark bound states and their properties are described by the Bethe-Salpeter equation in the pole approximation

$$1 - 2G_s \Pi_M(k^2)|_{k^2=M_M^2} = 0, \quad M = \pi, \sigma,$$

with the polarization operator $\Pi_M(k^2)$ determining the meson properties being defined as

$$\Pi_M(k^2) = i \int \frac{d^4p}{(2\pi)^4} \text{Tr} [\Gamma_M S(p+k) \Gamma_M S(p)],$$

where the vertex factor Γ_M depends on the meson species $M = \pi, \sigma, \rho$ and a_1 . For the pseudo-scalar π meson $\Gamma_\pi = i\gamma_5 \tau^a$ and for the scalar σ meson $\Gamma_\sigma = 1\tau^a$; $S(q)$ is the quark propagator and the trace is being taken over color, flavor and spinor indices.

For mesons at rest ($P = 0$) in the medium, these conditions correspond to the equations:

$$1 + 8G_s N_c N_f \int \frac{d^3p}{(2\pi)^3} \frac{1}{E_p} \frac{E_p^2}{M_\pi^2 - 4E_p^2} (1 - f(E^+) - f(E^-)) = 0,$$

$$1 + 8G_s N_c N_f \int \frac{d^3p}{(2\pi)^3} \frac{1}{E_p} \frac{E_p^2 - m^2}{M_\sigma^2 - 4E_p^2} (1 - f(E^+) - f(E^-)) = 0.$$

Both pion-quark $g_{\pi qq}(T, \mu)$ and sigma-quark $g_{\sigma qq}(T, \mu)$ coupling strengths can be defined from Π_M by the residuum of the mass pole approximation

$$g_{Mqq}^{-2}(T, \mu) = \frac{\partial \Pi_M(k^2)}{\partial k^2} \Big|_{k^2=M_M^2}, \quad M = \pi, \sigma.$$

Generally, the pole mass equation can be extended to the vector and axial-vector case and the set of equation together for the vector meson is solved self-consistently.

The mass of the ρ -meson and its width can be calculated as

$$\begin{aligned}
 M_\rho^2 &= \frac{g_{\rho qq}^2}{4G_V}, \\
 g_{\rho qq} &= \sqrt{6}g_{\sigma qq}, \\
 \Gamma_{\rho\pi\pi} &= \frac{g_{\rho\pi\pi}^2}{48\pi M_\rho^2} \sqrt{(M_\rho^2 - 4M_\pi^2)^3}.
 \end{aligned}$$

The decay width $\Gamma_{\sigma\pi\pi}$ within the NJL model is defined by the triangle Feynman diagram treating the sigma meson as quark-antiquark system

$$\Gamma_{\sigma\pi\pi} = \frac{3}{2} \frac{(2g_{\sigma qq}g_{\pi qq}^2 A_{\sigma\pi\pi}(T, \mu))^2}{16\pi M_\sigma} \sqrt{1 - \frac{4M_\pi^2}{M_\sigma^2}},$$

where the factor $3/2$ takes into account the isospin conservation and $g_{\sigma qq}$ and $g_{\pi qq}$ are coupling constants . The amplitude of the triangle vertex $A_{\sigma \rightarrow \pi\pi}$ is

$$A_{\sigma\pi\pi} = \int \frac{d^4q}{(2\pi)^4} \text{Tr}\{S(q) \Gamma_\pi S(q + P) \Gamma_\pi S(q)\}.$$

The kinematic factor $\sqrt{1 - 4M_\pi^2/M_\sigma^2}$ in leads to the constraint $M_\sigma > 2M_\pi$, if this condition is broken, the decay $\sigma \rightarrow \pi\pi$ is forbidden and the σ meson becomes a good bound state of the $\pi\pi$ interaction with only a negligible electromagnetic decay width from the $\sigma \rightarrow \gamma\gamma$ process

In order to describe the mass spectra in the NJL model, a set of parameters is required. Since we are interested in a phenomenology for the case that the constituent quark mass in the vacuum is $m = 400$ MeV, we choose the corresponding parameterization with the cutoff parameter $\Lambda = 0.5879$ GeV, the current quark mass $m_0 = 5.582$ MeV and the scalar-pseudoscalar coupling constant $G_s \Lambda^2 = 2.442$. The vector meson coupling constant $G_v \Lambda^2 = 2.4$ is found from fitting the ρ meson mass in vacuum $M_\rho = 780$ MeV.

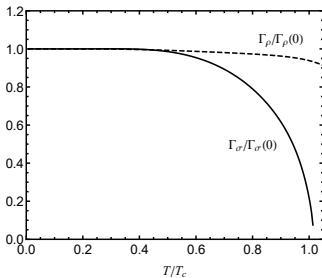
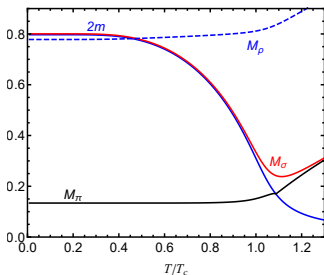


Figure 1: Left panel: the temperature dependence $M_i(T)$ of mass spectra for mesons ($i = \pi, \sigma, \rho$) and doubled quark mass $m(T)$. Right panel: scaled temperature dependence of total decay widths $\Gamma_i(T)/\Gamma_i(0)$ for mesons ($i = \sigma, \rho$) calculated within NJL model.

The temperature dependencies for $\Gamma_{\sigma\pi\pi}$ and $\Gamma_{\rho\pi\pi}$, calculated also in the framework of the NJL model. It can be seen that the $\sigma \rightarrow \pi\pi$ decay is forbidden after $T_{\text{diss}}^{\sigma} = 0.228$ GeV, where $\Gamma_{\sigma\pi\pi}$ drops to zero.

The phase shift δ_0^0 calculated for the temperatures $T = 0, 0.15, 0.185$ GeV is shown in left panel of Fig. 2. The blue line corresponds to the case without T-dependence and the results almost coincide due to the choice of the NJL parameters giving the mass $M_{\sigma} \sim 0.8$ GeV. The phase shift δ_0^2 calculated for the temperatures $T = 0, 0.15, 0.185$ GeV is shown in the right panel of Fig. 2. The solid blue line reproduces the scattering length approximation $\delta_0^2 = -0.12q/m_{\pi}$.

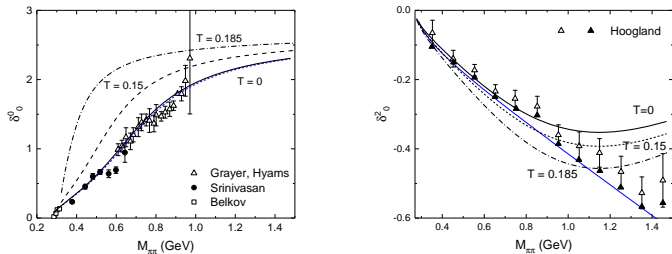


Figure 2: The phase shifts δ_0^0 (left panel) and δ_0^2 (right panel) for different temperatures $T = 0, 0.15, 0.185$ GeV. The solid blue line in the right panel corresponds to the scattering length approximation $\delta_0^2 = -0.12q/M_\pi$. The experimental data are taken from V. Srinivasan, Phys. Rev. D, 12 (681) 1975 .

The partial contributions to the total pressure are presented in the left panel of the Fig. 3 as functions of the temperature. The contributions from δ_0^0 and $5\delta_0^2$ compensate each other and the main virial correction to the pressure is given by the ρ meson. The pressure of the ideal pion gas (red dashed line) and the interacting pion gas (black solid line) are presented in the right panel of Fig. 3.

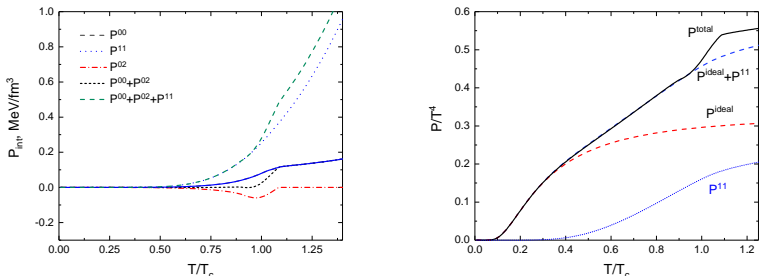


Figure 3: Left panel: Contributions to the pressure of the pion gas at second order of the virial expansion ($\pi\pi$ scattering) using the Beth-Uhlenbeck equation with medium dependent phase shifts. The quark Pauli blocking term P^{02} (blue solid line) is modified to take into account that it vanishes when the pion bound state is dissociated. Right panel: Pressure of the ideal pion gas (red dashed line), compared to the total pressure with all three interaction channels (black solid line) and with just the ρ -meson channel (blue dotted line). The ρ -meson contribution is also shown separately by the blue dash-dotted line.

The contribution to the pressure from the S-wave channel is small due to an approximate cancellation of the attractive ($I = 0$) sigma resonance contribution against the repulsive ($I = 2$) contribution that is explained by quark Pauli blocking. Using the simple Breit-Wigner approximation for the meson phase shifts and the nonrelativistic potential model result for the phase shift in the repulsive channel ($I=2$) together with the temperature dependence of the mass spectra from the NJL model, we show that this cancellation appears not only in low-energy and low-temperature region, but also takes place at finite temperature as long as $T \lesssim 0.75T_c$.

In Table 1 the relation $a_0^0/(5a_2^0)$ obtained in the frame of NJL model for different temperatures is shown.

Table 1: The relation $a_0^0/(5a_2^0)$ in the frame of NJL model.

	T=0	T = 0.14	T = 0.16	T = 0.19	T = 0.2
a_0^0	0.148	0.155	0.164	0.202	0.237
a_2^0	-0.036	-0.037	-0.037	-0.041	-0.043
$a_0^0/(5a_2^0)$	-0.826	-0.85	-0.88	-0.996	-1.11

Results obtained in the Table and results are shown in the Fig. show that the cancellation works also at finite temperature. At high temperatures near the phase transition the difference $P^{00} + 5P^{20}$ becomes finite and σ -meson channel should be taken into account.

That singularity in scattering lengths appears near the T_c due to the cancellation of the input from the σ -exchange diagram to the total amplitude. Near the critical temperature there appears the interplay between the pion Pauli blocking process and the creation of σ meson as a bounding state just before turning back into resonance state.

In the hadronization region for $T \approx T_c$, however, it is important to take into account the σ meson as the degree of freedom, since there it is a good resonance and the quark Pauli blocking ceases because of the Mott dissociation of the pion.

The NJL values $\Gamma_\sigma = 0.146$ GeV and $M_\sigma = 0.644$ GeV are comparable to theoretical researches in quark meson model, the functional approach and the non-local model which can be combined as $\Gamma_\sigma = 0.15$ - 0.173 GeV and $M_\sigma = 0.42$ - 0.587 GeV, but differ from the nonlocal model with a separable interaction kernel, where $\Gamma_\sigma = 0.456$ GeV at $M_\sigma = 0.762$ GeV and experimental results $\Gamma_{\sigma \rightarrow \pi\pi} = 282_{-50}^{+77}$ MeV at $M_\sigma = 390_{-36}^{+60}$ MeV (BES Collaboration) and $\Gamma_{\sigma \rightarrow \pi\pi} = 324_{-42}^{+40} \pm 21$ MeV with $M_\sigma = 478_{-23}^{+24} \pm 17$ MeV (The E791 Collaboration at Fermilab). The best fit of the experimental data is obtained for $M_\sigma = 0.8$ GeV, which is unavailable within the NJL model, where M_σ lies at the threshold $2m$.

The 'horn': experiments

Firstly, the "horn" was described by the NA49 Collaboration (NA49 Collaboration, PRC 66, 054902, 2002) and then it was shown that data can be placed on the same curve (STAR, AGS)

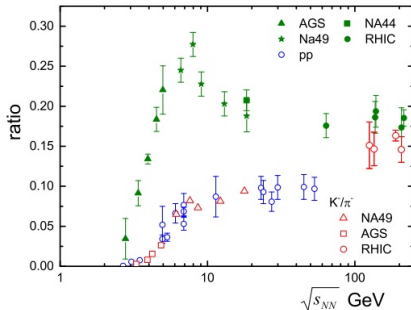


Figure 4: The K^+/π^+ and K^-/π^- ratio as the $\sqrt{s_{NN}}$

The 'horn': theoretical overview

- **the statistical model**: hadron resonances + σ - meson (implies the existence of the critical temperature for hadrons, **the hadron phase transition**) \Rightarrow the qualitative reproduction of the peak (Andronic PLB 673, 142 (2009)).
- **the SMES (the Statistical Model of Early Stages)**: a jump in the ratio is a result of the **deconfinement transition**: when deconfinement transition occurs the strangeness yield becomes independent of energy in the QGP ($m_s \rightarrow m_{s0}$) (M. Gazdzicki, M.I. Gorenstein, Acta Phys. Pol. B 30, 2705 (1999)).
- **the microscopic transport model**: with the hadron phase only can not reproduce experimental data (W. Ehehalt and W. Cassing, NPA602, 449 (1996); W. Cassing, E. L. Bratkovskaya, PR 308, 65 (1999); H. Petersen et al arXiv:0805.0567 [hep-ph]....)
- **the microscopic transport model + the partial restoration of chiral symmetry** (A. Palmese, et al. PRC 94, 044912 (2016): the quick increase in the K^+/π^+ appears as a result of **the partial chiral symmetry restoration**; the decrease is a result of QGP formation.

Propose of the work: use the SU(3) PNJL model

The Lagrangian (P. Costa et al. PRD79, 116003 (2009); E. Blanquier J. Phys. G: NPP 38, 105003 (2011)):

$$\mathcal{L} = \bar{q} (i\gamma^\mu D_\mu - \hat{m} - \gamma_0\mu) q + \frac{1}{2} G_s \sum_{a=0}^8 [(\bar{q} \lambda^a q)^2 + (\bar{q} i\gamma_5 \lambda^a q)^2] \\ + K \{ \det [\bar{q} (1 + \gamma_5) q] + \det [\bar{q} (1 - \gamma_5) q] \} - \mathcal{U}(\Phi, \bar{\Phi}; T)$$

$D_\mu = \partial^\mu - iA^\mu$, where A^μ is the gauge field with $A^0 = -iA_4$ and $A^\mu(x) = G_s A_a^\mu \frac{\lambda_a}{2}$
 The effective potential has to reproduce the Lattice calculation in the pure gauge sector:

$$\frac{\mathcal{U}(\Phi, \bar{\Phi}; T)}{T^4} = -\frac{b_2(T)}{2} \bar{\Phi}\Phi - \frac{b_3}{6} (\Phi^3 + \bar{\Phi}^3) + \frac{b_4}{4} (\bar{\Phi}\Phi)^2, \\ b_2(T) = a_0 + a_1 \left(\frac{T_0}{T}\right) + a_2 \left(\frac{T_0}{T}\right)^2 + a_3 \left(\frac{T_0}{T}\right)^3.$$

We can:

Propose of the work: use the SU(3) PNJL model

The Lagrangian (P. Costa et al. PRD79, 116003 (2009); E. Blanquier J. Phys. G: NPP 38, 105003 (2011)):

$$\mathcal{L} = \bar{q} (i\gamma^\mu D_\mu - \hat{m} - \gamma_0\mu) q + \frac{1}{2} G_s \sum_{a=0}^8 [(\bar{q} \lambda^a q)^2 + (\bar{q} i\gamma_5 \lambda^a q)^2] \\ + K \{ \det [\bar{q} (1 + \gamma_5) q] + \det [\bar{q} (1 - \gamma_5) q] \} - \mathcal{U}(\Phi, \bar{\Phi}; T)$$

$D_\mu = \partial^\mu - iA^\mu$, where A^μ is the gauge field with $A^0 = -iA_4$ and $A^\mu(x) = G_s A_a^\mu \frac{\lambda_a}{2}$
 The effective potential has to reproduce the Lattice calculation in the pure gauge sector:

$$\frac{\mathcal{U}(\Phi, \bar{\Phi}; T)}{T^4} = -\frac{b_2(T)}{2} \bar{\Phi}\Phi - \frac{b_3}{6} (\Phi^3 + \bar{\Phi}^3) + \frac{b_4}{4} (\bar{\Phi}\Phi)^2, \\ b_2(T) = a_0 + a_1 \left(\frac{T_0}{T}\right) + a_2 \left(\frac{T_0}{T}\right)^2 + a_3 \left(\frac{T_0}{T}\right)^3.$$

We can:

- explain and describe spontaneous chiral symmetry broken as $m_q = m_0 + \langle \bar{q}q \rangle$;

Propose of the work: use the SU(3) PNJL model

The Lagrangian (P. Costa et al. PRD79, 116003 (2009); E. Blanquier J. Phys. G: NPP 38, 105003 (2011)):

$$\mathcal{L} = \bar{q} (i\gamma^\mu D_\mu - \hat{m} - \gamma_0\mu) q + \frac{1}{2} G_s \sum_{a=0}^8 [(\bar{q} \lambda^a q)^2 + (\bar{q} i\gamma_5 \lambda^a q)^2] \\ + K \{ \det [\bar{q} (1 + \gamma_5) q] + \det [\bar{q} (1 - \gamma_5) q] \} - \mathcal{U}(\Phi, \bar{\Phi}; T)$$

$D_\mu = \partial^\mu - iA^\mu$, where A^μ is the gauge field with $A^0 = -iA_4$ and $A^\mu(x) = G_s A_a^\mu \frac{\lambda_a}{2}$
 The effective potential has to reproduce the Lattice calculation in the pure gauge sector:

$$\frac{\mathcal{U}(\Phi, \bar{\Phi}; T)}{T^4} = -\frac{b_2(T)}{2} \bar{\Phi}\Phi - \frac{b_3}{6} (\Phi^3 + \bar{\Phi}^3) + \frac{b_4}{4} (\bar{\Phi}\Phi)^2, \\ b_2(T) = a_0 + a_1 \left(\frac{T_0}{T}\right) + a_2 \left(\frac{T_0}{T}\right)^2 + a_3 \left(\frac{T_0}{T}\right)^3.$$

We can:

- explain and describe spontaneous chiral symmetry broken as $m_q = m_0 + \langle \bar{q}q \rangle$;
- simulate the confinement/deconfinement transition

Propose of the work: use the SU(3) PNJL model

The Lagrangian (P. Costa et al. PRD79, 116003 (2009); E. Blanquier J. Phys. G: NPP 38, 105003 (2011)):

$$\mathcal{L} = \bar{q} (i\gamma^\mu D_\mu - \hat{m} - \gamma_0\mu) q + \frac{1}{2} G_s \sum_{a=0}^8 [(\bar{q} \lambda^a q)^2 + (\bar{q} i\gamma_5 \lambda^a q)^2] \\ + K \{ \det [\bar{q} (1 + \gamma_5) q] + \det [\bar{q} (1 - \gamma_5) q] \} - \mathcal{U}(\Phi, \bar{\Phi}; T)$$

$D_\mu = \partial^\mu - iA^\mu$, where A^μ is the gauge field with $A^0 = -iA_4$ and $A^\mu(x) = G_s A_a^\mu \frac{\lambda_a}{2}$
 The effective potential has to reproduce the Lattice calculation in the pure gauge sector:

$$\frac{\mathcal{U}(\Phi, \bar{\Phi}; T)}{T^4} = -\frac{b_2(T)}{2} \bar{\Phi}\Phi - \frac{b_3}{6} (\Phi^3 + \bar{\Phi}^3) + \frac{b_4}{4} (\bar{\Phi}\Phi)^2, \\ b_2(T) = a_0 + a_1 \left(\frac{T_0}{T}\right) + a_2 \left(\frac{T_0}{T}\right)^2 + a_3 \left(\frac{T_0}{T}\right)^3.$$

We can:

- explain and describe spontaneous chiral symmetry broken as $m_q = m_0 + \langle \bar{q}q \rangle$;
- simulate the confinement/deconfinement transition
- build the phase diagram with crossover at low chemical potential and 1st order transition at high chemical potential ($m_0 \neq 0$),

The mean-field approximation

The grand potential density:

$$\Omega = U(\Phi, \bar{\Phi}; T) + g_S \sum_{i=u,d,s} \langle \bar{q}_i q_i \rangle^2 + 4g_D \langle \bar{q}_u q_u \rangle \langle \bar{q}_d q_d \rangle \langle \bar{q}_s q_s \rangle - 2N_c \sum_{i=u,d,s} \int \frac{d^3p}{(2\pi)^3} E_i - 2T \sum_{i=u,d,s} \int \frac{d^3p}{(2\pi)^3} (N_{\Phi}^+(E_i) + N_{\bar{\Phi}}(E_i))$$

with the functions

$$N_{\Phi}^+(E_i) = \text{Tr}_c \left[\ln(1 + L^\dagger e^{-\beta(E_i - \mu_i)}) \right] = \left[1 + 3 \left(\Phi + \bar{\Phi} e^{-\beta E_i^+} \right) e^{-\beta E_i^+} + e^{-3\beta E_i^+} \right],$$

$$N_{\bar{\Phi}}(E_i) = \text{Tr}_c \left[\ln(1 + L e^{-\beta(E_i + \mu_i)}) \right] = \left[1 + 3 \left(\bar{\Phi} + \Phi e^{-\beta E_i^-} \right) e^{-\beta E_i^-} + e^{-3\beta E_i^-} \right],$$

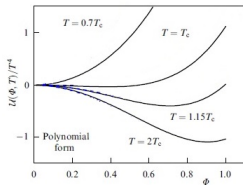
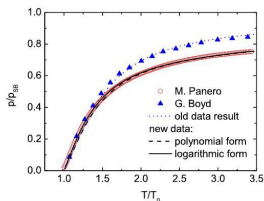
where $E_i^\pm = E_i \mp \mu_i$, $\beta = 1/T$, $E_i = \sqrt{p_i^2 + m_i^2}$ is the energy of quarks and $\langle \bar{q}_i q_i \rangle$ is the quark condensate.

The equations of motion

$$\frac{\partial \Omega}{\partial \sigma_f} = 0, \quad \frac{\partial \Omega}{\partial \Phi} = 0, \quad \frac{\partial \Omega}{\partial \bar{\Phi}} = 0.$$

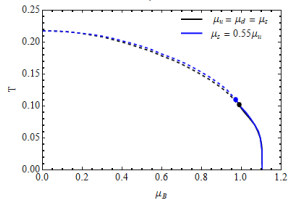
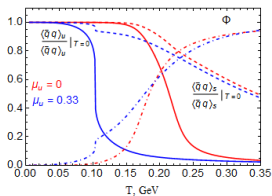
The model properties

The effective potential $\mathcal{U}(\Phi, \bar{\Phi}; T)$ properties



The chiral phase transition properties:

- a) $\mu_u = \mu_d = \mu_s$,
- b) $\mu_u = \mu_d; \mu_s = 0.55\mu_u$



Masses

The gap equation for quarks depends on the quark condensates:

$$m_i = m_{0i} - 2g_S \langle \bar{q}_i q_i \rangle - 2g_D \langle \bar{q}_j q_j \rangle \langle \bar{q}_k q_k \rangle,$$

The meson masses are defined by the Bethe-Salpeter equation at $P = 0$

$$1 - P_{ij} \Pi_{ij}^P(P_0 = M, P = 0) = 0,$$

with

$$P_\pi = G_s + K \langle \bar{q}_s q_s \rangle, \quad P_K = G_s + K \langle \bar{q}_u q_u \rangle$$

and the polarization operator:

$$\Pi_{ij}^P(P_0) = 4 \left((I_1^i + I_1^j) - [P_0^2 - (m_i - m_j)^2] I_2^{ij}(P_0) \right),$$

When $T > T_{\text{Mott}}$ ($P_0 > m_i + m_j$) \rightarrow the meson \rightarrow the resonance state \rightarrow the solution has to be defined in the form $P_0 = M_M - \frac{1}{2}i\Gamma_M$.

The mass spectra

$$\mu_u = \mu_d = \mu_s, \quad \mu_B = 3\mu_u, \quad \rho_B = (\rho_u + \rho_d + \rho_s)/3$$

To describe the mesons in dense matter, Fermi momentum λ_i , should be related with the chemical potential of quarks $\mu_i = \sqrt{\lambda_i^2 + m_i^2}$.

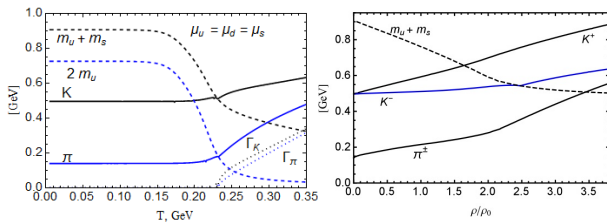
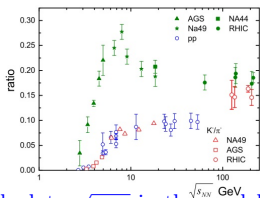


Figure 5: The mass spectra at zero and finite chemical potential (see for discussion P.Costa et al. PRD71 (2005) 116002)

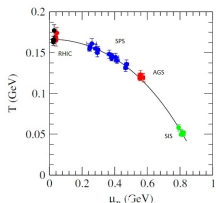
T- μ variables J. Cleymans et al.
 PRC73, 034905 (2006)

$$T(\mu_B) = a - b\mu_B^2 - c\mu_B^4, \quad \mu_B(\sqrt{s}) = \frac{d}{1 + e\sqrt{s}}$$

The experimental results



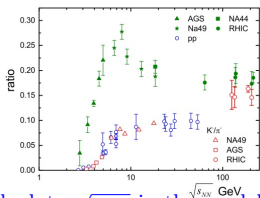
How calculate $\sqrt{s_{NN}}$ in the model?



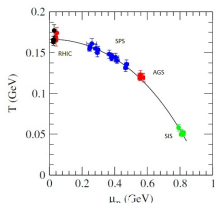
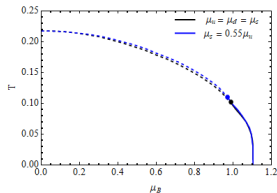
T- μ variables J. Cleymans et al.
 PRC73, 034905 (2006)

$$T(\mu_B) = a - b\mu_B^2 - c\mu_B^4, \quad \mu_B(\sqrt{s}) = \frac{d}{1 + e\sqrt{s}}$$

The experimental results



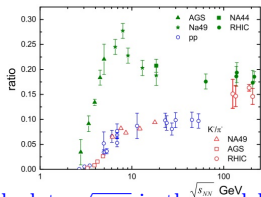
How calculate $\sqrt{s_{NN}}$ in the model?



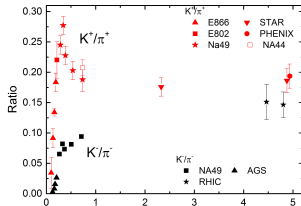
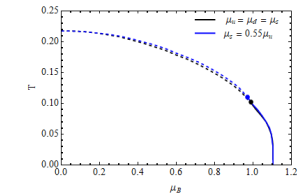
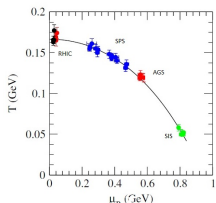
T- μ variables J. Cleymans et al.
 PRC73, 034905 (2006)

$$T(\mu_B) = a - b\mu_B^2 - c\mu_B^4, \quad \mu_B(\sqrt{s}) = \frac{d}{1 + e\sqrt{s}}$$

The experimental results



How calculate $\sqrt{s_{NN}}$ in the model?

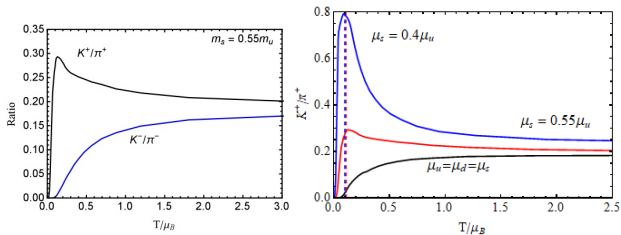


Kaon to pion ratio

$$n_{K^\pm} = \int_0^\infty p^2 dp \frac{1}{e^{(\sqrt{p^2 + m_{K^\pm}} \mp \mu_{K^\pm})} - 1},$$

$$n_{\pi^\pm} = \int_0^\infty p^2 dp \frac{1}{e^{(\sqrt{p^2 + m_{\pi^\pm}} \mp \mu_{\pi^\pm})} - 1}.$$

with parameter $\mu_\pi = 0.135$ (M. Kataja, P.V. Ruuskanen PLB 243, 181 (1990)) and $\mu_K = \mu_u - \mu_s$ (see for example A. Lavagno and D. Pigato, EPJ Web of Conferences 37, 09022 (2012)).



How we can improve the PNJL model? I

- introduce a phenomenological dependence of $G_s(\Phi)$ (Y. Sakai et al PRD 82, 076003 (2010), P. de Forcrand, O. Philipsen NPB 642, 290(2002), A. Friesen et al. IJMPA30, 1550089 (2015).)

$$\tilde{G}_s(\Phi) = G_s[1 - \alpha_1 \Phi \bar{\Phi} - \alpha_2 (\Phi^3 + \bar{\Phi}^3)]$$

with $\alpha_1 = \alpha_2 = 0.2$.

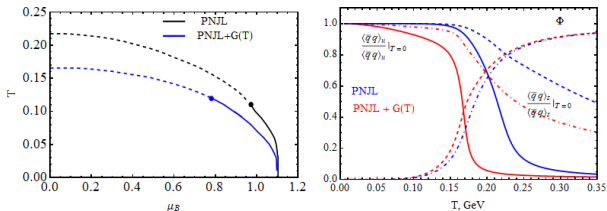


Figure 6: $\mu_s = 0.5\mu_u$

How we can improve the PNJL model? II

- the effect of axial symmetry and the coupling $K = K_0 \exp(-(\rho/\rho_0)^2)$ on the dense states see for discussion P. Costa et al AIP Conf.Proc. 775 (2005) 173; arXiv::0503258
- and introduce $G_s(\Phi)$ with $\alpha_1 = \alpha_2 = 0.2$.

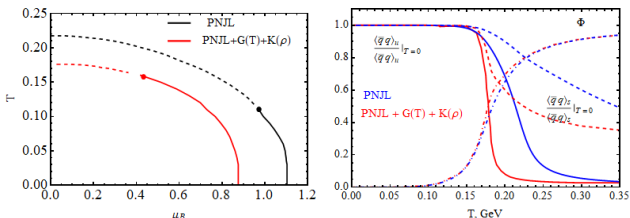
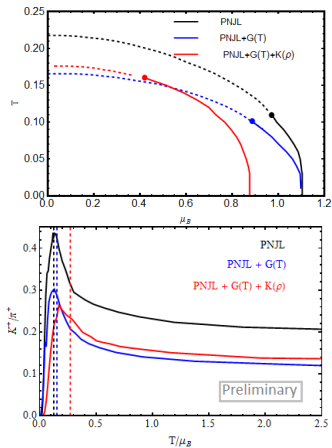
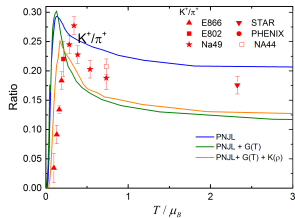


Figure 7: $\mu_s = 0.5\mu_u$

Results

Figure 8: $\mu_s = 0.5\mu_u$

Theory + experiment



Results and outlooks

- splitting of kaons masses at high densities \Rightarrow the difference in the behavior of the K/π at low energies.
- the height of the peak in the model depends on the properties of the matter (strange chemical potential, T and μ_B) - it looks like we need more realistic description of the media.
- the position of the peak pretends to be depend on curvature of phase diagram/CEP position. This statement can be checked more carefully, for example in the PNJL model with vector interaction, where at critical value of G_V first order transition can disappear.

Thank you for your attention